Rediscovering alignment relations with Graph Convolutional Networks

Pierre Monnin [a,*], Chedy Raïssi [a,b], Amedeo Napoli [a] and Adrien Coulet [a,c]
[a] *Université de Lorraine, CNRS, Inria, LORIA, F-54000 Nancy, France*
E-mails: pierre.monnin@loria.fr, chedy.raissi@inria.fr, amedeo.napoli@loria.fr, adrien.coulet@inria.fr
[b] *Ubisoft, Singapore*
E-mail: chedy.raissi@inria.fr
[c] *Université de Paris, Inria Paris, Inserm UMR1138, F-75012 Paris, France*
E-mail: adrien.coulet@inria.fr

Abstract. Knowledge graphs are concurrently published and edited in the Web of data. Hence they may overlap, which makes key the task that consists in matching their content. This task encompasses the identification, within and across knowledge graphs, of nodes that are equivalent, more specific, or weakly related. In this article, we propose to match nodes of a knowledge graph by *(i)* learning node embeddings with Graph Convolutional Networks such that similar nodes have low distances in the embedding space, and *(ii)* clustering nodes based on their embeddings. We experimented this approach on a biomedical knowledge graph and particularly investigated the interplay between formal semantics and GCN models with the two following main focuses. Firstly, we applied various inference rules associated with domain knowledge, independently or combined, before learning node embeddings, and we measured the improvements in matching results. Secondly, while our GCN model is agnostic to the exact alignment relations (*e.g.*, equivalence, weak similarity), we observed that distances in the embedding space are coherent with the "strength" of these different relations (*e.g.*, smaller distances for equivalences), somehow corresponding to their rediscovery by the model.

Keywords: Knowledge Graph, matching, embedding, Graph Convolutional Network, ontology, clustering

1. Introduction

In the Semantic Web paradigms [1], knowledge graphs offer both human and software agents the ability to publish, edit, access, and interpret data and knowledge. In such paradigms, agents work concurrently, which leads to different knowledge graphs describing similar units. The combined use of these knowledge graphs allows access to the full extent of the available knowledge, which is beneficial to many applications, such as fact-checking or query answering. For this conjoint use to be possible, one crucial task lies in *matching* units within and across knowledge graphs, *i.e.*, finding *alignments* or correspondences between, *e.g.*, nodes, edges, or subgraphs [2]. This task is well-studied in the *Ontology Matching* research field [2] and is challenging since knowledge graphs differ in quality, completeness, vocabularies, and languages. Consequently, different alignment relations may hold between units: some may indicate that two units are equivalent, weakly related, or that one is more specific than the other.

In the present work, we focus on matching nodes of a knowledge graph represented within Semantic Web standards [1]. We view such a knowledge graph as a directed and labeled multigraph in which nodes represent entities of a world (*e.g.*, places, drugs), literals (*e.g.*, dates, integers), or classes of individuals (*e.g.*, `Person`, `Drug`). Nodes are linked together through edges defined as triples ⟨`subject`, `predicate`, `object`⟩ in the Resource Description Format language, where the `predicate` qualifies the relationship holding between the `subject` and the `object` (*e.g.*, `has-side-effect`, `has-name`). Entities,

[*]Corresponding author. E-mail: pierre.monnin@loria.fr.

classes, and predicates are identified by Uniform Resource Identifiers (URIs). Knowledge graphs can be associated with ontologies, *i.e.*, formal representations of a domain [3], in which predicates and classes are organized into two hierarchies by a subsumption relation.

We propose to match nodes that represent entities through the approach outlined in Figure 1. This approach uses graph embeddings, *i.e.*, low-dimensional vectors that represent graph substructures (*e.g.*, nodes, edges, subgraphs) while preserving as much as possible the properties of the graph [4]. More precisely, we learn node embeddings with Graph Convolution Networks (GCNs) [5, 6] such that similar nodes have a low distance between their embeddings. We employ graph embeddings since their continuous nature may provide the needed flexibility to cope with the heterogeneous representations of nodes to match [7]. Additionally, GCNs compute the embedding of a node by considering the embeddings of its neighbors in the graph. Hence, nodes with similar neighborhoods will have similar embeddings, which is well-adapted to a structural and relational matching approach [8, 9].

To match nodes, we apply a clustering algorithm on the embedding space and consider nodes that belong to the same cluster as similar. These resulting clusters are evaluated by being compared with *gold clusters*, which we define as groups of nodes linked directly or indirectly through *similarity links* existing in the knowledge graph. Similarity links connect similar nodes and their predicate represent the alignment relation that holds between them. For example, nodes may be identical (`owl:sameAs` links), weakly similar (`skos:related` links), or one may be more specific than the other (`skos:broadMatch` links). Hence, our approach is supervised and requires the preexistence of such similarity links. Here, we use the results of a rule-based method [10] in a "knowledge graph as silver standard" perspective [11].

Within our approach, we particularly investigated the two following aspects. Firstly, we applied various inference rules associated with domain knowledge (*e.g.*, class and predicate hierarchies, symmetry of predicates), independently or combined, before learning node embeddings, and we measured the improvements in matching results. Secondly, as aforementioned, similarity links may represent different alignment relations. We made our GCN model agnostic to these exact relations during learning. However, we observed that distances between the embeddings of similar nodes are different and coherent with the "strength" of each alignment relation (*e.g.*, smaller distances for equivalences, larger distances for weak similarities). Such results allow us to think that the model is able to rediscover these alignment relations. To the best of our knowledge, our approach is the first one to investigate these aspects in a matching task using GCNs and clustering.

We experimented our work within the biomedical domain of pharmacogenomics (PGx), which studies the influence of genetic factors on drug response phenotypes. For example, Figure 2 depicts the relationship `pgr_1`, which states that patients treated with warfarin may experience vascular disorders because of variations in the CYP2C9 gene. PGx knowledge originates from distinct sources: reference databases such as PharmGKB [12], biomedical literature, or the mining of Electronic Health Records of hospitals. Consequently, there is an interest in matching these sources to obtain a consolidated view of the PGx knowledge. Such a view would certainly be beneficial to precision medicine, which aims at tailoring drug treatments to patients to reduce adverse effects and maximize drug efficacy [13, 14].

Additionally, PGx knowledge is well adapted to our matching approach based on GCNs. Indeed, PGx knowledge consists of *n*-ary relationships between drugs, genomic variations, and phenotypes. Only binary relations exist in Semantic Web standards. Thus, PGx relationships are reified as nodes whose neighbors are the involved drugs, genetic factors, and phenotypes (see Figure 2) [15]. In this context, matching PGx relationships reduces to matching the nodes resulting from their reification. By using GCNs, nodes representing PGx relationships that involve similar drugs, genetic factors, and phenotypes will have similar embeddings since they have similar neighborhoods.

The remainder of this paper is organized as follows. In Section 2, we outline some works related to node matching in knowledge graphs and graph embeddings. We detail the core of our matching approach (node embeddings and clustering) in Section 3, and how inference rules associated with domain knowledge are considered in Section 4. In Section 5, we experiment this approach on PGxLOD, a large knowledge graph we built that contains 50,435 PGx relationships [16]. Finally, we discuss our results and conclude in Section 6 and 7.

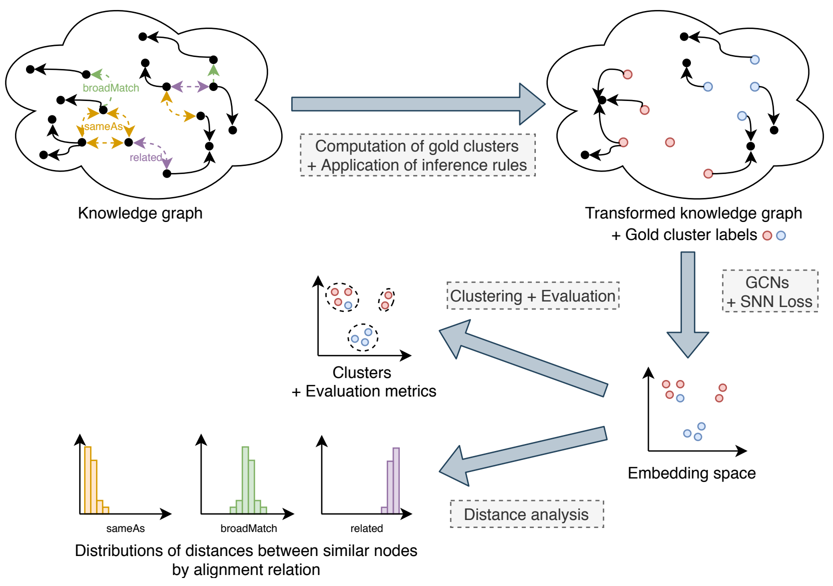

Fig. 1. Outline of our approach. Gold clusters are computed from existing *similarity links* in the knowledge graph (*e.g.*, `owl:sameAs`, `skos:broadMatch`, `skos:related`, etc.). These similarity links are then removed and various inferences rules associated with domain knowledge are applied on the knowledge graph. Embeddings of nodes are learned with Graph Convolutional Networks (GCNs) and the Soft Nearest Neighbor (SNN) loss. Clustering algorithms are then applied on the embedding space and the resulting clusters are evaluated with regard to the gold clusters. A distance analysis is also performed for each alignment relation.

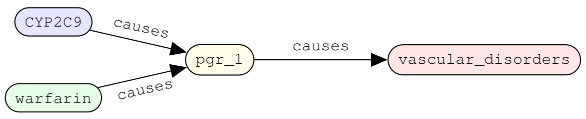

Fig. 2. Representation of a PGx relationship between gene `CYP2C9`, drug `warfarin` and phenotype `vascular_disorders`. This relationship is reified through the individual `pgr_1`, connecting its components through the `causes` predicate.

2. Related work

Numerous papers exist about knowledge graph and ontology matching. The interested reader could refer to the book of Euzenat and Shvaiko [2] for a formalization of the matching task, and a detailed presentation of the main methods. In the following, we focus on graph embedding techniques. Such techniques have been successfully applied on knowledge graphs for various tasks such as node classification, link prediction, or node clustering [4, 17]. Interestingly, the task of matching nodes can be alternatively tackled as a link prediction task (*i.e.*, predicting similarity links between nodes) or as a node clustering task (*i.e.*, grouping similar nodes into clusters). Here, we choose the node clustering approach.

Existing papers about graph embedding differ in the considered type of graphs (*e.g.*, homogeneous graphs, heterogeneous graphs such as knowledge graphs) or in the graph embedding techniques used (*e.g.*, matrix factorization, deep learning with or without random walk), as listed in the taxonomies of problems and techniques in the survey of Cai et al. [4]. Hereafter, a few specific examples are detailed but a more thorough overview can be found in the following surveys [4, 17, 18]. Some approaches are translational. For example, TransE [19] computes for each triple $\langle s, p, o \rangle$ of a knowledge graph, embeddings h_s, h_p, h_o, such that $h_s + h_p \approx h_o$, *i.e.*, the translation vector from the subject to the object of a triple corresponds to the embedding of the predicate. This approach is adapted for link prediction but, according to the authors, it is unclear if it can adequately model relations of distinct arities, such as *1-to-Many*, or *Many-to-Many*. Other approaches use random walks in the knowledge graph. For example, RDF2Vec [20] first extracts, for each node, a set of sequences of graph sub-structures starting from this node. Elements in these sequences can be edges, nodes, or subtrees. Then, sequences feed the word2vec model that compute embeddings for each element in a sequence by either maximizing the probability of an element given the other elements of the sequence (Continuous Bag of World architecture) or maximizing the probability of the other elements given the considered element (Skip-gram architecture).

The approach adopted in this article is based on Graph Convolutional Networks (GCNs). GCNs have been introduced for semi-supervised classification over graphs [5] and extended for entity classification and link prediction in knowledge graphs [6]. Contrasting TransE and RDF2Vec that work at the triple and sequence levels, GCNs compute the embedding of a node by considering its neighborhood in the graph. Hence, as aforementioned, we believe GCNs are well-suited for our application of matching reified *n*-ary relationships since similar relationships have similar neighborhoods. Other existing works rely on this assumption that similar nodes have similar neighborhoods and use GCNs for their matching. For example, Wang et al. [9] propose to align cross-lingual knowledge graphs by using GCNs to learn node embeddings such that nodes representing the same entity in different languages have close embeddings. Pang et al. [8] use the same approach to align two knowledge graphs, but introduce an iterative aspect. Some newly-aligned entities are selected and used when learning embeddings in the next iteration. To avoid introducing false positive alignments, the newly-aligned entities are selected with a distance-based criteria proposed by the authors. Interestingly, the two previous approaches take into account literals during the embedding process and use the *triplet loss*, also used by TransE. On the contrary, in our work, we discard literals and use the *Soft Nearest Neighbor loss* [21] to consider all positive and negative examples instead of sampling[1].

However, previous methods do not consider inference rules associated with domain knowledge represented in knowledge graphs on the contrary of recent papers [22]. For example, Logic Tensor Networks [23] learn groundings of logical terms and logical clauses. The grounding of a logical term consists in a vector of real numbers (*i.e.*, an embedding) and the grounding of a logical clause is a real number in the interval $[0, 1]$ (*i.e.*, the confidence in the truth of the clause). The learning process aims at minimizing the satisfiability error of a set of clauses, while ensuring the logical reasoning. This work can interestingly be compared to graph embeddings if knowledge graphs are considered in their logical form, *i.e.*, considering nodes as logical terms and edges linking two nodes as logical formulae. Alternatively, Wang et al. [24] propose an hybrid attention mechanism named "Logic Attention Network" (LAN) to use in embedding approaches for link prediction. LAN combines a mechanism based on logical rules and a neural network mechanism. The rule-based mechanism weights neighbors by promoting those linked by a predicate that has been found to strongly imply the predicate of the link to predict. Besides implications between predicates, more complex logical rules can be associated with knowledge graphs through ontologies. That is why Gutiérrez-Basulto and Schockaert [25] investigate how to ensure logical consistency through geometrical constraints on embedding spaces and if classical embedding techniques respect such constraints.

These related works and our preliminary results [26] inspired the present work where we investigate how *(i)* inference rules associated with domain knowledge can improve the performances in node matching and *(ii)* the distributions of distances in the embedding space can correspond to a "rediscovery" of the alignment relations.

3. Matching nodes with Graph Convolutional Networks and clustering

3.1. Approach outline

Our approach is outlined in Figure 1. It takes as input a knowledge graph $\mathcal{K}$ and a set S of nodes to match, where S is a subset of the nodes of $\mathcal{K}$. To illustrate, in our biomedical application, we only intend to match nodes that represent reified PGx relationships. We discard literals and edges incident to literals from $\mathcal{K}$ and S. Hence, a node is either an entity or a class. We consider that we have at our disposal *gold clusters*, *i.e.*, sets of nodes from S that are already labeled as similar. These gold clusters can have uneven sizes. We propose to match nodes in S as follows:

1. Learn embeddings for all nodes in $\mathcal{K}$ such that nodes in S labeled as similar (*i.e.*, belonging to the same gold cluster) have smaller distances between their embeddings (Subsection 3.2).
2. Apply a clustering algorithm on the embedding space and consider nodes belonging to the same cluster as similar (Subsection 3.3).

[1]GCNs and the Soft Nearest Neighbor loss are further detailed in Subsection 3.2

It should be noted that gold clusters can result from another automatic matching method or a manual alignment by an expert. For example, in Section 5, our gold clusters are computed from similarity links semi-automatically obtained with rules manually written by experts [10]. As aforementioned, these similarity links can represent different alignment relations (*e.g.*, equivalence, weak similarity). We further detail in Subsection 5.1 how these different relations are taken into account in our experiments.

3.2. *Learning node embeddings with Graph Convolutional Networks and the Soft Nearest Neighbor loss*

To learn embeddings for all nodes in $\mathcal{K}$, we propose to use Graph Convolutional Networks (GCNs) and the Soft Nearest Neighbor loss. In the following, we adopt the notations and definitions of Schlichtkrull et al. [6]. As such, $\mathcal{R}$ denotes the set of predicates in the considered knowledge graph $\mathcal{K}$. Given a node i and a predicate $r \in \mathcal{R}$, we denote by $\mathcal{N}_i^r$ the set of nodes reachable from i by an edge labeled by r.

Graph Convolutional Networks (GCNs) can be seen as a message-passing framework of multiple layers, in which the embedding $h_i^{(l+1)}$ of a node i at layer $(l+1)$ depends on the embeddings of its neighbors at level (l), as stated in Eq. (1).

$$h_i^{(l+1)} = \sigma\left(\sum_{r\in\mathcal{R}}\sum_{j\in\mathcal{N}_i^r}\frac{1}{c_{i,r}}W_r^{(l)}h_j^{(l)} + W_0^{(l)}h_i^{(l)}\right) \tag{1}$$

This convolution over the neighboring nodes j of i is computed with a specific weight matrix $W_r^{(l)}$ for each predicate $r \in \mathcal{R}$ and each layer (l). The convolution is regularized by a constant $c_{i,r}$, that can be set for each node and each predicate. Similarly to Schlichtkrull et al. [6], we use $c_{i,r} = |\mathcal{N}_i^r|$. The weight matrix $W_0^{(l)}$ enables a self-connection, *i.e.*, the embedding of i at layer $(l+1)$ also depends on its embedding at layer (l). σ is a non-linear function such as ReLU or tanh.

The number of predicates in $\mathcal{K}$ can lead to a high number of parameters $W_r^{(l)}$ to optimize. That is why we use the basis-decomposition proposed by Schlichtkrull et al. [6]. Hence, each $W_r^{(l)}$ is decomposed as follows:

$$W_r^{(l)} = \sum_{b=1}^{B} a_{rb}^{(l)} V_b^{(l)} \tag{2}$$

For each level (l), B matrices $V_b^{(l)} \in \mathbb{R}^{d^{(l+1)}\times d^{(l)}}$ and $|\mathcal{R}| \times B$ coefficients $a_{rb}^{(l)} \in \mathbb{R}$ are learned, where $d^{(l)}$ and $d^{(l+1)}$ denote the dimension of embeddings at level (l) and level $(l+1)$ respectively. Then, each $W_r^{(l)}$ is computed as a linear combination of matrices $V_b^{(l)}$ and coefficients $a_{rb}^{(l)}$. As only these coefficients depend on predicates r, the number of parameters to learn is reduced.

In our objective of clustering similar nodes, we propose to train GCNs by minimizing the Soft Nearest Neighbor (SNN) loss defined by Frosst et al. [21] and presented in Eq. (3).

$$\mathcal{L}_{\text{SNN}} = -\frac{1}{|N|}\sum_{i\in N}\log\left(\frac{\sum\limits_{\substack{j\in N\\ j\neq i\\ Y_i=Y_j}} e^{-\frac{||h_i-h_j||^2}{T}}}{\sum\limits_{\substack{k\in N\\ k\neq i}} e^{-\frac{||h_i-h_k||^2}{T}}}\right) \tag{3}$$

The input of the SNN loss consists of:

- A set N of nodes belonging to the gold clusters (see Subsection 5.2).
- A set Y of labels for nodes in N. These labels corresponds to the assignments of nodes in N to the gold clusters.
- A temperature T.
- Embeddings h of nodes. These embeddings are the output of the last layer of the GCN model.

Minimizing the SNN loss corresponds to minimizing intra-cluster distances and maximizing inter-cluster distances for the gold clusters of nodes in N. The temperature T determines how distances influence the loss. Indeed, distances between widely separated embeddings are taken into account when T is large whereas only distances between close embeddings are taken into account when T is small. To avoid T as an hyperparameter of the model, we adopt the same learning procedure as Frosst et al. [21]: T is initialized to a predefined value and is optimized by learning $\frac{1}{T}$ as a model parameter.

The computation of $\mathcal{L}_{\text{SNN}}$ (Eq. (3)) considers all positive and negative examples from N. Indeed, distances between nodes with the same label are minimized (*i.e.*, positive examples) whereas distances between nodes with different labels are maximized (*i.e.*, negative examples). However, it is noteworthy that $\mathcal{K}$ is based on the *Open World Assumption*. Hence, nodes with different labels are regarded as dissimilar (*i.e.*, negative examples) while their (dis)similarity may only be unknown.

3.3. Matching nodes by clustering their embeddings

After embeddings of all nodes in the graph have been learned and output by the last layer of GCNs, we perform a clustering on embeddings h_i for all nodes $i \in S$, *i.e.*, all nodes to match. Nodes that belong to the same predicted cluster are considered as similar and these predicted clusters are compared and evaluated with regard to gold clusters.

Here, we experiment with the three distinct clustering algorithms presented in Table 1. Their choice was motivated by their availability in scikit-learn [27]. Interestingly, these algorithms differ in their parameters: they take either the number of clusters to find or the minimum size of clusters. This difference allows us to evaluate the influence of inference rules associated with domain knowledge in different settings (see Section 4). To compare predicted clusters with gold clusters, we use the three usual metrics presented in Table 2.

4. Evaluating the influence of applying inference rules associated with domain knowledge

Semantic Web knowledge graphs are represented within formalims such as Description Logics [29] that are equipped with inference rules. Hence, we propose to evaluate the improvements in the results of our matching approach (detailed in Section 3) when considering such inference rules, independently or combined. Here, we only consider the following logic axioms: class and predicate assertions, equivalence axioms between entities or classes, subsumption axioms between classes or predicates, and axioms defining predicate inverses. Accordingly, we generate six different graphs by running over $\mathcal{K}$ the inference rules associated with these different axioms until saturation. Then, we test our approach on each of these six graphs. These graphs are summarized in Table 3 and further described below.

$\mathcal{G}_0$ constitutes the baseline in which no inference rules are run and with the systematic addition of abstract inverses. Indeed, Schlichtkrull et al. [6] consider that for every predicate $r \in \mathcal{R}$, there exists an inverse $r_{\text{inv}} \in \mathcal{R}$. Thus, for every $r \in \mathcal{R}$, we add an abstract inverse $r_{\text{inv}} \in \mathcal{R}$ such that its adjacency matrix represents the inverse of r. This addition of abstract inverses is performed in all other graphs, except when explicitly stated otherwise. $\mathcal{G}_1$ results from the contraction of `owl:sameAs` edges. Indeed, in $\mathcal{K}$, several nodes representing the same entity can co-exist. In this case, they may be linked (directly or indirectly) by `owl:sameAs` edges and should be considered as one, which is enabled by this contraction. In $\mathcal{G}_2$, we do not always add abstract inverses but consider definitions of inverses and symmetry of predicates instead. That is to say:

(i) For a predicate r_1 defined as symmetric (*i.e.*, $r_1 \equiv r_1^{-1}$), we do not add an abstract inverse $r_{1\ \text{inv}}$ and complete its adjacency matrix to ensure its symmetry.
(ii) For a predicate r_2 that has a defined inverse r_3 (*i.e.*, $r_3 \equiv r_2^{-1}$), we do not add an abstract inverse $r_{2\ \text{inv}}$ and complete their adjacency matrices to ensure they represent inverse predicates.
(iii) Otherwise, for a predicate r_4 that neither is symmetric nor have a defined inverse, we add an abstract inverse $r_{4\,\text{inv}}$ such that its adjacency matrix represents the inverse of r_4.

$\mathcal{G}_3$ takes into account the hierarchy of predicates. Indeed, if a predicate r_1 is a subpredicate of r_2 (*i.e.*, $r_1 \sqsubseteq r_2$) and a triple $\langle i, r_1, j\rangle$ exists, then we make sure the triple $\langle i, r_2, j\rangle$ also exists in the graph. This completion is performed by considering the transitive closure of the subsumption relation $\sqsubseteq$. That is to say, if $r_1 \sqsubseteq r_2$ and $r_2 \sqsubseteq r_3$, we also consider $r_1 \sqsubseteq r_3$. Similarly, $\mathcal{G}_4$ completes `type` edges based on the hierarchy of ontology classes defined by `subClassOf` edges. Hence, if $\langle i, \texttt{type}, j\rangle$ and $\langle j, \texttt{subClassOf}, k\rangle$ exist in the graph, then we ensure that $\langle i, \texttt{type}, k\rangle$ is also in the graph. Here again, `subClassOf` edges are considered by computing their transitive closure. Finally, $\mathcal{G}_5$ is the graph resulting from all transformations from $\mathcal{G}_1$ to $\mathcal{G}_4$.

5. Experiments

We experimented with PGxLOD[2], a large knowledge graph about pharmacogenomics (PGx) that we previously built [16]. Our approach is implemented in Python, using PyTorch and the Deep Graph Library for learning embeddings, and scikit-learn for clustering. Our code is available on GitHub[3].

[2]https://pgxlod.loria.fr
[3]https://github.com/pmonnin/gcn-matching

Table 1

Clustering algorithms applied on the embeddings of nodes in S. Nodes that belong to the same predicted cluster are considered as similar.

Algorithm	Parameter	Description
Ward	Number of clusters to find	Hierarchical clustering algorithm that successively merges clusters by minimizing the variance of merged clusters
Single	Number of clusters to find	Hierarchical clustering algorithm that successively merges clusters whose distance between their closest observations is minimal
OPTICS [28]	Minimum size of clusters	Algorithm that finds zones of high density and expand clusters from them

Table 2

Performance metrics used to compare the clusters predicted by the algorithms presented in Table 1 with gold clusters.

Metric	Abbr.	Domain	Description
Unsupervised Clustering Accuracy	ACC	$[0, 1]$	Counts nodes whose predicted cluster label is the same as their gold cluster label divided by the total number of nodes. As labels may be permuted between predicted and gold clusters, the mapping with the best ACC is used.
Adjusted Rand Index	ARI	$[-1, 1]$	Considers all pairs of nodes and counts those whose nodes are assigned to the same or different clusters both in predicted and gold clusters. ARI is equal to 0 for a random labeling, and equal to 1 for a perfect labeling (up to a permutation). ARI is adjusted for chance.
Normalized Mutual Information	NMI	$[0, 1]$	Measures the mutual information between the predicted and gold clusters, normalized by the entropy of both types of clusters. NMI is equal to 1 for a perfect labeling (up to a permutation).

Table 3

Visual summary of the transformations of $\mathcal{K}$ to evaluate the influence of the application of inference rules associated with domain knowledge on node matching. $\mathcal{G}_0$ is the baseline that corresponds to no inference rules being run and the systematic addition of abstract inverses.

Graph	Before	After
$\mathcal{G}_0$	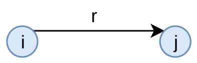	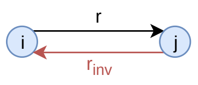
$\mathcal{G}_1$	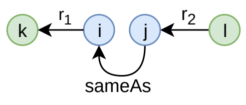	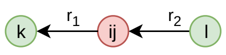
$\mathcal{G}_2$	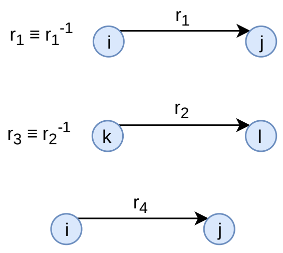	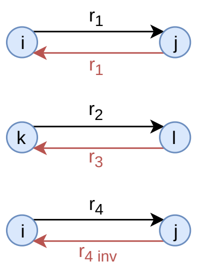
$\mathcal{G}_3$	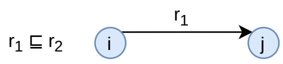	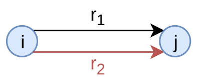
$\mathcal{G}_4$	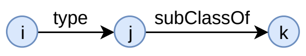	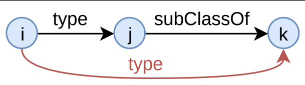
$\mathcal{G}_5$	All transformations from $\mathcal{G}_1$ to $\mathcal{G}_4$	

5.1. Knowledge graph and gold clusters of similar nodes

We chose to use PGxLOD as the input knowledge graph of our approach since it presents several needed characteristics. First, PGxLOD contains nodes whose matching is well-adapted to a structure-based approach such as ours. Additionally, alignments are expected to be found between these nodes. Indeed, PGxLOD contains 50,435 PGx relationships resulting from:

- an automatic extraction from the reference database PharmGKB;
- an automatic extraction from the biomedical literature;
- a manual representation of 10 studies made from Electronic Health Records of hospitals.

Alignments are expected to be found between such relationships since, for example, PharmGKB is manually curated by experts after a literature review. Recall that PGx relationships are *n*-ary, and thus they are reified as nodes, as illustrated in Figure 2 [15]. Hence, nodes representing these relationships form our set S of nodes to match. The reification process entails that neighbors of such nodes are the drugs, genetic factors, and phenotypes involved in the relationships. Consequently, similar relationships have similar neighborhoods, which makes a structure-based approach such as ours well-adapted for their matching.

Second, PGxLOD contains `owl:sameAs` edges (or equivalence axioms), which makes possible the transformation represented in $\mathcal{G}_1$. Indeed, PGxLOD integrates several Linked Open Data sets: ClinVar, DrugBank, SIDER, DisGeNET, PharmGKB, and CTD. These LOD sets contain facts describing components of PGx relationships (*i.e.*, drugs, phenotypes, and genetic factors). Several LOD sets may describe the same entities and we know it explicitly, *i.e.*, some nodes belonging to different LOD sets are linked with `owl:sameAs` edges. For example, this could be the case of a drug represented both in PharmGKB and DrugBank. Thus, we can apply the `owl:sameAs` identification.

Third, PGxLOD contains subsumption axioms between classes and between predicates, which makes possible the transformations represented in $\mathcal{G}_3$ and $\mathcal{G}_4$. Indeed, PGxLOD includes the ATC, MeSH, PGxO, and ChEBI ontologies.

Fourth, some PGx relationships in S are already labeled as similar through similarity links. These links use the five following alignment relations: `owl:sameAs`, `skos:closeMatch`, `skos:relatedMatch`, `skos:related`, and `skos:broadMatch`. Links using `owl:sameAs` and `skos:closeMatch` indicate strong similarities, whereas `skos:relatedMatch` and `skos:related` indicate weaker similarities. Links using `skos:broadMatch` indicate that a PGx relationship is more specific than another. These links result from the application of five matching rules [10] and are removed before running inference rules over $\mathcal{K}$, learning embeddings, and clustering. However, they allow to compute *gold clusters*, *i.e.*, sets of nodes that are considered as similar since they are directly or indirectly connected through similarity links. These gold clusters are used to evaluate our approach in a "knowledge graph as silver standard" perspective [11]. We propose the different *gold clusterings* detailed in Table 4. They variously consider the five alignment relations to evaluate our approach in different settings (*e.g.*, all the different alignment relations in $\mathcal{C}_0$, only symmetric relations in $\mathcal{C}_1$, only equivalences in $\mathcal{C}_2$). For each gold clustering, gold clusters correspond to the connected components computed by only considering the (undirected) similarity links of the selected alignment relations between nodes in S. Hence, all alignment relations are regarded as symmetric (undirected links) and transitive (connected components), which is coherent with the majority of alignment relations (see Table 4). Figure 3 presents the sizes of the resulting gold clusters. We notice that many gold clusters have a size lower or equal to 10, and that considering `skos:related` or `skos:broadMatch` links increases the maximal size of gold clusters. The availability of all these different alignment relations also allows to perform the distance analysis described in Subsection 5.4 and indicated in Figure 1.

5.2. Learning node embeddings

We experimented our approach with different pairs $(\mathcal{C}_i, \mathcal{G}_j)$ that were selected for their experimental interest. All gold clusterings were experimented with graphs $\mathcal{G}_0$ and $\mathcal{G}_5$ to have a global view of the impact on performance of applying inference rules associated with domain knowledge. All graphs were experimented with $\mathcal{C}_0$ to have a finer evaluation of each inference rule on the most heterogeneous gold clustering. For each experimented pair $(\mathcal{C}_i, \mathcal{G}_j)$, a 5-fold cross-validation was performed as follows. For each $\mathcal{C}_i$, S is split into five sets S^i_k ($k \in \{1,2,3,4,5\}$). All S^i_k contain the same number of nodes for each gold cluster of $\mathcal{C}_i$ larger than 5 nodes. Each set S^i_k is successively

Table 4

Alignment relations considered in each gold clustering to compute the gold clusters used in our experiments. We indicate whether a relation is transitive (T or ¬ T) and symmetric (S or ¬ S).

	`owl:sameAs`	`skos:closeMatch`	`skos:relatedMatch`	`skos:related`	`skos:broadMatch`
	T, S	T, S	T, S	¬ T, S	T, ¬ S
$\mathcal{C}_0$	×	×	×	×	×
$\mathcal{C}_1$	×	×	×	×	
$\mathcal{C}_2$	×				
$\mathcal{C}_3$		×			
$\mathcal{C}_4$			×		
$\mathcal{C}_5$				×	
$\mathcal{C}_6$					×

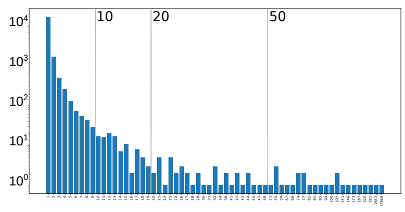

(a) $\mathcal{C}_0$ (max $= 17,568$)

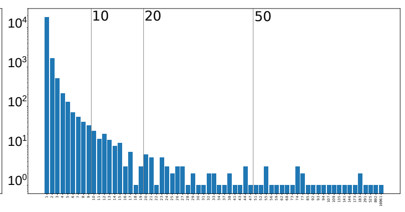

(b) $\mathcal{C}_1$ (max $= 16,961$)

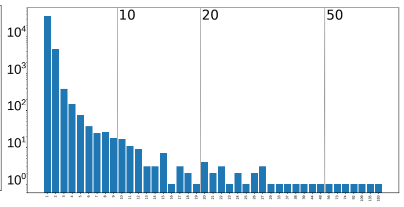

(c) $\mathcal{C}_2$ (max $= 183$)

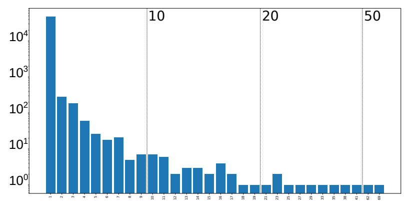

(d) $\mathcal{C}_3$ (max $= 69$)

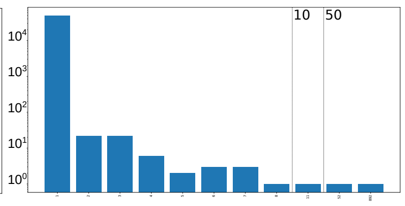

(e) $\mathcal{C}_4$ (max $= 892$)

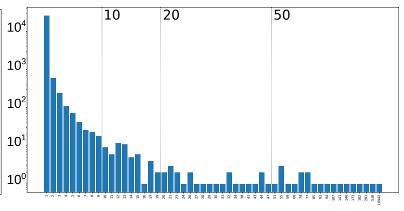

(f) $\mathcal{C}_5$ (max $= 16,942$)

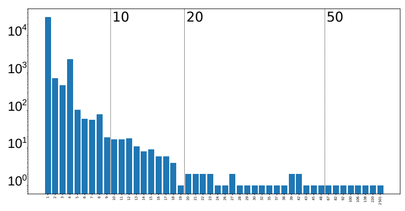

(g) $\mathcal{C}_6$ (max $= 2,501$)

Fig. 3. Number of gold clusters (y-axis) by size (x-axis) for each gold clustering. The max value is the maximum size of gold clusters (in terms of number of nodes). The minimum size is 1 for every gold clustering. Only gold clusters larger than 10, 20, and 50 nodes are later used to compute performance metrics. Gold clusterings are defined in Table 4.

used as the test set S_{test}, while set $S^i_{(k+1)}$ is used as the validation set S_{val}[4]. Remaining sets form the train set S_{train}.

An architecture formed by 3 GCN layers is used to learn node embeddings. The input layer consists in a featureless approach as in [5, 6], *i.e.*, the input is just a one-hot vector for each node of the graph. All three layers have an output dimension of 16. Therefore, output embeddings for all nodes in the knowledge graph are in $\mathbb{R}^{16}$. The activation function used on the input and hidden layers is tanh while the output layer uses a linear function. We use a basis-decomposition of 10 bases and set $c_{i,r} = |\mathcal{N}_i^r|$ for all i and all r. In such a 3-layer architecture, it follows from Eq. (1) that only neighboring nodes up to 3 hops[5] of nodes in S will have an impact on their embeddings, output at layer 3. Thus, to save memory, we reduce graphs to such 3-hop neighborhoods. Statistics about these reduced graphs are available in Table 5.

Only the embeddings of nodes in S (here, the PGx relationships) are considered in our clustering task. Hence, only these embeddings are constrained in the SNN loss. However, in $\mathcal{L}_{\text{SNN}}$ (Eq. (3)), each node needs at least one other node assigned to the same gold cluster (*i.e.*, having the same label). Thus, only gold clusters of size greater or equal to 10 are used in the learning process since each S^i_k contains at least 2 nodes of these clusters. This is particularly needed for the validation and test losses but we chose to use the same constraint for the train loss for homogeneity. We use the Adam optimizer [30] with a starting learning rate of 0.01. T is initialized to 1. We learn during 200 epochs with an early-stopping mechanism: if the validation loss does not decrease of 0.0001 after 10 epochs, the learning process is stopped.

5.3. Clustering

Clustering algorithms are only applied on the embeddings of nodes in S_{test} since they are the nodes we aim to match. Recall that the learning process only considers nodes belonging to gold clusters whose size is greater or equal to 10. Accordingly, we apply the three clustering algorithms introduced in Table 1 and evaluate their performance on embeddings of nodes in S_{test} that belong to gold clusters whose size is greater or equal to 50, 20, and 10. These different sizes allow to evaluate the influence of inference rules in the performance of our matching approach when considering only large or all gold clusters.

Results on all gold clusterings and graphs $\mathcal{G}_0$ and $\mathcal{G}_5$ are displayed in Table 6, Table 7 and Table 8. In these tables, gray cells indicate the best results among clustering algorithms given a gold clustering, a graph, and a metric. For example, in Table 6, considering $\mathcal{C}_0$ and $\mathcal{G}_0$, the best ACC is obtained with the Single clustering algorithm. Underlined values indicate the best result between $\mathcal{G}_0$ and $\mathcal{G}_5$ given a gold clustering and a metric. For example, in Table 6, given $\mathcal{C}_1$, the best NMI for Ward is obtained with $\mathcal{G}_0$ whereas the best ACC is obtained with $\mathcal{G}_5$. We notice that applying all inference rules (*i.e.*, $\mathcal{G}_5$) generally increases performance for $\mathcal{C}_0$ and $\mathcal{C}_1$ whereas results for the other gold clusterings do not show such an homogeneous and important increase in performance.

Results on $\mathcal{C}_0$ and all graphs are displayed in Table 9, Table 10, and Table 11. In these tables, gray cells indicate the best result among clustering algorithms and underlined values indicate the best result between graphs. For example, in Table 9, given $\mathcal{G}_0$, the best ACC is obtained with the Single clustering algorithm. Given the Single algorithm, the best ARI is obtained with $\mathcal{G}_3$ and $\mathcal{G}_5$. Here again, we notice that applying all inference rules (*i.e.*, $\mathcal{G}_5$) leads to the best results. However, computing all instantiations based on the transitive closure of the subsumption (*i.e.*, $\mathcal{G}_4$) seems to degrade clustering performance.

Table 5
Statistics of PGxLOD and its transformations as described in Section 4. Statistics for PGxLOD discard literals and edges incident to literals. As we use a 3-layer architecture, statistics for all $\mathcal{G}_i$ only consider neighboring nodes up to 3 hops of nodes in S (*i.e.*, PGx relationships to match). # denotes “number of”.

	# nodes	# edges	# predicates
PGxLOD	11,808,396	43,341,712	416
$\mathcal{G}_0$	3,758,814	39,956,844	689
$\mathcal{G}_1$	3,879,081	46,960,365	733
$\mathcal{G}_2$	3,758,814	22,085,701	347
$\mathcal{G}_3$	3,758,814	41,048,190	697
$\mathcal{G}_4$	3,758,928	42,691,984	701
$\mathcal{G}_5$	3,882,945	27,277,789	375

[4]S^i_1 is the validation set when $S_{\text{test}} = S^i_5$.

[5]The 3-hop neighborhood of a node n consists of all the nodes that can be reached with a breadth-first traversal that starts at n and traverses at most 3 edges.

Table 6

Results of clustering nodes that belong to gold clusters whose size is greater or equal to 50 for graphs $\mathcal{G}_0$ and $\mathcal{G}_5$. Average and standard deviation for each metric are computed on test folds during a 5-fold cross validation. Given a gold clustering, gray cells indicate the best results among clustering algorithms and underlined values indicate the best result between $\mathcal{G}_0$ and $\mathcal{G}_5$.

		$\mathcal{G}_0$			$\mathcal{G}_5$		
		ACC	ARI	NMI	ACC	ARI	NMI
$\mathcal{C}_0$	Ward	0.24 ± 0.02	0.07 ± 0.01	$\underline{0.37 \pm 0.01}$	$\underline{0.25 \pm 0.02}$	0.07 ± 0.01	0.35 ± 0.01
	Single	0.84 ± 0.08	0.66 ± 0.13	0.59 ± 0.05	$\underline{0.90 \pm 0.00}$	$\underline{0.75 \pm 0.01}$	$\underline{0.64 \pm 0.02}$
	OPTICS	0.61 ± 0.05	0.21 ± 0.08	0.25 ± 0.04	$\underline{0.68 \pm 0.02}$	$\underline{0.27 \pm 0.05}$	$\underline{0.27 \pm 0.02}$
$\mathcal{C}_1$	Ward	0.19 ± 0.02	0.05 ± 0.00	$\underline{0.33 \pm 0.01}$	$\underline{0.20 \pm 0.03}$	0.05 ± 0.01	0.31 ± 0.01
	Single	0.85 ± 0.01	0.55 ± 0.04	0.51 ± 0.03	0.85 ± 0.01	$\underline{0.57 \pm 0.03}$	0.51 ± 0.03
	OPTICS	0.64 ± 0.03	0.19 ± 0.03	0.28 ± 0.01	$\underline{0.71 \pm 0.04}$	$\underline{0.26 \pm 0.06}$	$\underline{0.30 \pm 0.02}$
$\mathcal{C}_2$	Ward	0.88 ± 0.03	0.84 ± 0.03	0.94 ± 0.01	0.88 ± 0.03	0.84 ± 0.03	0.94 ± 0.01
	Single	$\underline{0.88 \pm 0.03}$	$\underline{0.84 \pm 0.03}$	$\underline{0.94 \pm 0.01}$	0.86 ± 0.04	0.81 ± 0.07	0.93 ± 0.02
	OPTICS	$\underline{0.94 \pm 0.06}$	$\underline{0.92 \pm 0.07}$	$\underline{0.97 \pm 0.03}$	0.91 ± 0.06	0.88 ± 0.08	0.95 ± 0.04
$\mathcal{C}_3$	Ward	0.52 ± 0.01	0.00 ± 0.00	0.00 ± 0.00	$\underline{0.53 \pm 0.01}$	0.00 ± 0.00	0.00 ± 0.00
	Single	0.53 ± 0.01	0.00 ± 0.00	0.00 ± 0.00	0.53 ± 0.01	0.00 ± 0.00	0.00 ± 0.00
	OPTICS	1.00 ± 0.00	1.00 ± 0.00	1.00 ± 0.00	1.00 ± 0.00	1.00 ± 0.00	1.00 ± 0.00
$\mathcal{C}_4$	Ward	0.94 ± 0.00	0.00 ± 0.00	0.00 ± 0.00	0.94 ± 0.00	0.00 ± 0.00	0.00 ± 0.00
	Single	0.94 ± 0.00	0.00 ± 0.00	0.00 ± 0.00	0.94 ± 0.00	0.00 ± 0.00	0.00 ± 0.00
	OPTICS	$\underline{0.45 \pm 0.14}$	-0.02 ± 0.06	0.08 ± 0.08	0.38 ± 0.11	$\underline{0.01 \pm 0.05}$	$\underline{0.11 \pm 0.08}$
$\mathcal{C}_5$	Ward	$\underline{0.20 \pm 0.02}$	$\underline{0.04 \pm 0.00}$	$\underline{0.24 \pm 0.01}$	0.15 ± 0.02	0.03 ± 0.00	0.20 ± 0.01
	Single	0.88 ± 0.00	$\underline{0.31 \pm 0.03}$	$\underline{0.29 \pm 0.03}$	$\underline{0.89 \pm 0.00}$	0.30 ± 0.03	0.27 ± 0.02
	OPTICS	$\underline{0.71 \pm 0.03}$	$\underline{0.18 \pm 0.07}$	$\underline{0.18 \pm 0.04}$	0.68 ± 0.06	0.07 ± 0.07	0.11 ± 0.04
$\mathcal{C}_6$	Ward	0.69 ± 0.02	0.48 ± 0.03	0.64 ± 0.03	$\underline{0.76 \pm 0.12}$	$\underline{0.58 \pm 0.22}$	$\underline{0.67 \pm 0.12}$
	Single	$\underline{0.86 \pm 0.02}$	$\underline{0.60 \pm 0.09}$	$\underline{0.63 \pm 0.08}$	0.82 ± 0.02	0.46 ± 0.12	0.52 ± 0.11
	OPTICS	$\underline{0.59 \pm 0.07}$	$\underline{0.21 \pm 0.09}$	0.44 ± 0.06	0.58 ± 0.05	0.19 ± 0.06	$\underline{0.45 \pm 0.04}$

Table 7

Results of clustering nodes that belong to gold clusters whose size is greater or equal to 20 for graphs $\mathcal{G}_0$ and $\mathcal{G}_5$. Average and standard deviation for each metric are computed on test folds during a 5-fold cross validation. Given a gold clustering, gray cells indicate the best results among clustering algorithms and underlined values indicate the best result between $\mathcal{G}_0$ and $\mathcal{G}_5$.

		$\mathcal{G}_0$			$\mathcal{G}_5$		
		ACC	ARI	NMI	ACC	ARI	NMI
$\mathcal{C}_0$	Ward	0.17 ± 0.01	0.04 ± 0.00	$\underline{0.32 \pm 0.01}$	0.17 ± 0.02	0.04 ± 0.00	0.31 ± 0.01
	Single	0.79 ± 0.08	0.64 ± 0.11	0.54 ± 0.05	$\underline{0.86 \pm 0.01}$	$\underline{0.69 \pm 0.01}$	$\underline{0.57 \pm 0.01}$
	OPTICS	0.45 ± 0.03	0.09 ± 0.02	0.17 ± 0.01	$\underline{0.50 \pm 0.01}$	$\underline{0.13 \pm 0.01}$	$\underline{0.19 \pm 0.01}$
$\mathcal{C}_1$	Ward	0.15 ± 0.01	0.03 ± 0.00	$\underline{0.31 \pm 0.01}$	0.15 ± 0.01	0.03 ± 0.00	0.30 ± 0.00
	Single	0.64 ± 0.22	0.38 ± 0.19	0.45 ± 0.06	$\underline{0.82 \pm 0.01}$	$\underline{0.58 \pm 0.03}$	$\underline{0.52 \pm 0.03}$
	OPTICS	0.47 ± 0.02	0.08 ± 0.01	0.20 ± 0.01	$\underline{0.51 \pm 0.02}$	$\underline{0.11 \pm 0.03}$	0.20 ± 0.01
$\mathcal{C}_2$	Ward	0.98 ± 0.00	0.98 ± 0.02	0.99 ± 0.00	0.98 ± 0.00	$\underline{0.99 \pm 0.01}$	0.99 ± 0.00
	Single	0.97 ± 0.03	0.95 ± 0.05	0.98 ± 0.01	$\underline{0.98 \pm 0.00}$	$\underline{0.98 \pm 0.01}$	$\underline{0.99 \pm 0.00}$
	OPTICS	0.69 ± 0.01	0.44 ± 0.04	0.78 ± 0.01	$\underline{0.73 \pm 0.03}$	$\underline{0.48 \pm 0.04}$	$\underline{0.81 \pm 0.02}$
$\mathcal{C}_3$	Ward	$\underline{0.92 \pm 0.06}$	$\underline{0.89 \pm 0.08}$	$\underline{0.95 \pm 0.03}$	0.89 ± 0.05	0.84 ± 0.08	0.93 ± 0.03
	Single	$\underline{0.91 \pm 0.05}$	$\underline{0.87 \pm 0.06}$	$\underline{0.95 \pm 0.03}$	0.88 ± 0.07	0.84 ± 0.09	0.93 ± 0.04
	OPTICS	0.89 ± 0.07	0.87 ± 0.08	0.94 ± 0.08	$\underline{0.92 \pm 0.06}$	$\underline{0.90 \pm 0.09}$	$\underline{0.95 \pm 0.04}$
$\mathcal{C}_4$	Ward	0.94 ± 0.00	0.00 ± 0.00	0.00 ± 0.00	0.94 ± 0.00	0.00 ± 0.00	0.00 ± 0.00
	Single	0.94 ± 0.00	0.00 ± 0.00	0.00 ± 0.00	0.94 ± 0.00	0.00 ± 0.00	0.00 ± 0.00
	OPTICS	0.29 ± 0.05	0.01 ± 0.01	0.09 ± 0.02	$\underline{0.34 \pm 0.05}$	$\underline{0.03 \pm 0.01}$	$\underline{0.11 \pm 0.02}$
$\mathcal{C}_5$	Ward	$\underline{0.12 \pm 0.01}$	$\underline{0.02 \pm 0.00}$	$\underline{0.21 \pm 0.01}$	0.10 ± 0.00	0.01 ± 0.00	0.17 ± 0.00
	Single	0.85 ± 0.01	$\underline{0.32 \pm 0.09}$	$\underline{0.28 \pm 0.06}$	$\underline{0.86 \pm 0.00}$	0.20 ± 0.03	0.27 ± 0.02
	OPTICS	0.48 ± 0.02	0.05 ± 0.01	$\underline{0.10 \pm 0.01}$	$\underline{0.52 \pm 0.02}$	0.05 ± 0.02	0.09 ± 0.01
$\mathcal{C}_6$	Ward	$\underline{0.56 \pm 0.05}$	$\underline{0.39 \pm 0.10}$	$\underline{0.67 \pm 0.02}$	0.50 ± 0.06	0.29 ± 0.08	0.65 ± 0.03
	Single	0.64 ± 0.07	0.43 ± 0.13	0.62 ± 0.05	$\underline{0.78 \pm 0.01}$	$\underline{0.67 \pm 0.06}$	$\underline{0.71 \pm 0.03}$
	OPTICS	0.44 ± 0.03	0.08 ± 0.03	$\underline{0.38 \pm 0.02}$	$\underline{0.47 \pm 0.05}$	0.08 ± 0.08	0.37 ± 0.05

Table 8

Results of clustering nodes that belong to gold clusters whose size is greater or equal to 10 for graphs $\mathcal{G}_0$ and $\mathcal{G}_5$. Average and standard deviation for each metric are computed on test folds during a 5-fold cross validation. Given a gold clustering, gray cells indicate the best results among clustering algorithms and underlined values indicate the best result between $\mathcal{G}_0$ and $\mathcal{G}_5$.

			$\mathcal{G}_0$			$\mathcal{G}_5$	
		ACC	ARI	NMI	ACC	ARI	NMI
$\mathcal{C}_0$	Ward	$\underline{0.14 \pm 0.01}$	0.02 ± 0.00	$\underline{0.29 \pm 0.01}$	0.13 ± 0.01	0.02 ± 0.00	0.28 ± 0.02
	Single	0.66 ± 0.17	0.53 ± 0.22	0.52 ± 0.06	$\underline{0.74 \pm 0.15}$	$\underline{0.61 \pm 0.16}$	$\underline{0.54 \pm 0.06}$
	OPTICS	0.25 ± 0.02	0.02 ± 0.01	$\underline{0.12 \pm 0.01}$	$\underline{0.27 \pm 0.01}$	$\underline{0.03 \pm 0.01}$	0.11 ± 0.01
$\mathcal{C}_1$	Ward	0.13 ± 0.01	0.01 ± 0.00	$\underline{0.28 \pm 0.01}$	$\underline{0.14 \pm 0.01}$	0.01 ± 0.00	0.27 ± 0.01
	Single	0.41 ± 0.12	0.18 ± 0.07	0.41 ± 0.02	$\underline{0.72 \pm 0.15}$	$\underline{0.53 \pm 0.14}$	$\underline{0.52 \pm 0.04}$
	OPTICS	0.28 ± 0.01	0.02 ± 0.00	0.13 ± 0.01	0.28 ± 0.00	0.02 ± 0.00	0.13 ± 0.01
$\mathcal{C}_2$	Ward	0.99 ± 0.00	0.99 ± 0.00	0.99 ± 0.00	0.99 ± 0.00	0.99 ± 0.00	0.99 ± 0.00
	Single	0.99 ± 0.01	0.99 ± 0.02	0.99 ± 0.00	0.99 ± 0.00	0.99 ± 0.00	0.99 ± 0.00
	OPTICS	$\underline{0.63 \pm 0.01}$	$\underline{0.31 \pm 0.01}$	$\underline{0.67 \pm 0.01}$	0.62 ± 0.01	0.29 ± 0.01	0.66 ± 0.01
$\mathcal{C}_3$	Ward	$\underline{0.92 \pm 0.00}$	$\underline{0.90 \pm 0.10}$	$\underline{0.94 \pm 0.05}$	0.86 ± 0.04	0.81 ± 0.05	0.89 ± 0.02
	Single	$\underline{0.90 \pm 0.07}$	$\underline{0.88 \pm 0.12}$	$\underline{0.93 \pm 0.05}$	0.83 ± 0.05	0.77 ± 0.08	0.88 ± 0.04
	OPTICS	$\underline{0.75 \pm 0.02}$	$\underline{0.58 \pm 0.03}$	$\underline{0.78 \pm 0.02}$	0.72 ± 0.03	0.49 ± 0.07	0.73 ± 0.05
$\mathcal{C}_4$	Ward	0.99 ± 0.00	0.90 ± 0.07	0.86 ± 0.08	0.99 ± 0.00	$\underline{0.91 \pm 0.05}$	$\underline{0.88 \pm 0.04}$
	Single	0.98 ± 0.01	0.83 ± 0.10	0.78 ± 0.15	$\underline{0.99 \pm 0.00}$	$\underline{0.88 \pm 0.05}$	$\underline{0.85 \pm 0.07}$
	OPTICS	0.18 ± 0.03	$\underline{0.01 \pm 0.01}$	0.06 ± 0.01	0.18 ± 0.01	0.00 ± 0.00	0.06 ± 0.01
$\mathcal{C}_5$	Ward	$\underline{0.09 \pm 0.01}$	0.01 ± 0.00	$\underline{0.18 \pm 0.01}$	0.07 ± 0.00	0.01 ± 0.00	0.14 ± 0.01
	Single	0.81 ± 0.01	0.31 ± 0.12	0.25 ± 0.08	$\underline{0.82 \pm 0.01}$	$\underline{0.32 \pm 0.08}$	$\underline{0.26 \pm 0.05}$
	OPTICS	0.27 ± 0.01	0.01 ± 0.00	$\underline{0.06 \pm 0.01}$	$\underline{0.28 \pm 0.01}$	0.01 ± 0.01	0.05 ± 0.01
$\mathcal{C}_6$	Ward	$\underline{0.48 \pm 0.03}$	$\underline{0.24 \pm 0.05}$	$\underline{0.64 \pm 0.01}$	0.44 ± 0.02	0.16 ± 0.03	0.60 ± 0.02
	Single	0.63 ± 0.07	0.56 ± 0.14	0.70 ± 0.04	$\underline{0.74 \pm 0.02}$	$\underline{0.76 \pm 0.05}$	$\underline{0.76 \pm 0.03}$
	OPTICS	0.37 ± 0.02	0.02 ± 0.01	0.29 ± 0.02	0.37 ± 0.02	$\underline{0.03 \pm 0.01}$	0.29 ± 0.01

Table 9

Results of clustering nodes that belong to gold clusters whose size is greater or equal to 50 for $\mathcal{C}_0$ and all graphs. Average and standard deviation for each metric are computed on test folds during a 5-fold cross validation. Gray cells indicate the best result among clustering algorithms. Underlined values indicate the best result between graphs. $\downarrow$ indicates a lower value with regard to $\mathcal{G}_0$.

		Ward	Single	OPTICS
$\mathcal{G}_0$	ACC	0.24 ± 0.02	0.84 ± 0.08	0.61 ± 0.05
	ARI	0.07 ± 0.01	0.66 ± 0.13	0.21 ± 0.08
	NMI	$\underline{0.37 \pm 0.01}$	0.59 ± 0.05	0.25 ± 0.04
$\mathcal{G}_1$	ACC	0.24 ± 0.02	0.86 ± 0.00	$\downarrow$ 0.58 ± 0.03
	ARI	0.07 ± 0.01	0.70 ± 0.02	$\downarrow$ 0.16 ± 0.03
	NMI	$\downarrow$ 0.35 ± 0.02	$\downarrow$ 0.58 ± 0.02	$\downarrow$ 0.23 ± 0.01
$\mathcal{G}_2$	ACC	0.24 ± 0.01	0.89 ± 0.02	$\underline{0.70 \pm 0.01}$
	ARI	0.07 ± 0.00	0.72 ± 0.03	$\underline{0.32 \pm 0.03}$
	NMI	$\downarrow$ 0.34 ± 0.01	0.61 ± 0.04	$\underline{0.28 \pm 0.01}$
$\mathcal{G}_3$	ACC	$\downarrow$ 0.22 ± 0.03	0.89 ± 0.02	0.63 ± 0.03
	ARI	0.07 ± 0.01	$\underline{0.75 \pm 0.02}$	0.29 ± 0.04
	NMI	$\downarrow$ 0.36 ± 0.01	0.63 ± 0.03	$\underline{0.28 \pm 0.02}$
$\mathcal{G}_4$	ACC	$\downarrow$ 0.23 ± 0.02	$\downarrow$ 0.80 ± 0.16	0.62 ± 0.02
	ARI	0.07 ± 0.01	$\downarrow$ 0.63 ± 0.21	$\downarrow$ 0.20 ± 0.03
	NMI	$\downarrow$ 0.36 ± 0.01	$\downarrow$ 0.58 ± 0.08	$\downarrow$ 0.24 ± 0.01
$\mathcal{G}_5$	ACC	$\underline{0.25 \pm 0.02}$	$\underline{0.90 \pm 0.00}$	0.68 ± 0.02
	ARI	0.07 ± 0.01	$\underline{0.75 \pm 0.01}$	0.27 ± 0.05
	NMI	$\downarrow$ 0.35 ± 0.01	$\underline{0.64 \pm 0.02}$	0.27 ± 0.02

Table 10

Results of clustering nodes that belong to gold clusters whose size is greater or equal to 20 for $\mathcal{C}_0$ and all graphs. Average and standard deviation for each metric are computed on test folds during a 5-fold cross validation. Gray cells indicate the best result among clustering algorithms. Underlined values indicate the best result between graphs. $\downarrow$ indicates a lower value with regard to $\mathcal{G}_0$.

			Ward		Single		OPTICS
	ACC		0.17 ± 0.01		0.79 ± 0.08		0.45 ± 0.03
$\mathcal{G}_0$	ARI		$\underline{0.04 \pm 0.00}$		0.64 ± 0.11		0.09 ± 0.02
	NMI		$\underline{0.32 \pm 0.01}$		0.54 ± 0.05		0.17 ± 0.01
	ACC		$\underline{0.19 \pm 0.01}$		0.81 ± 0.01	$\downarrow$	0.43 ± 0.02
$\mathcal{G}_1$	ARI		$\underline{0.04 \pm 0.00}$		0.64 ± 0.02	$\downarrow$	0.07 ± 0.03
	NMI		$\underline{0.32 \pm 0.01}$	$\downarrow$	0.52 ± 0.01	$\downarrow$	0.16 ± 0.02
	ACC		0.17 ± 0.01		0.81 ± 0.08		0.48 ± 0.01
$\mathcal{G}_2$	ARI		$\underline{0.04 \pm 0.00}$	$\downarrow$	0.63 ± 0.09		0.11 ± 0.02
	NMI	$\downarrow$	0.30 ± 0.01		0.54 ± 0.05		0.17 ± 0.01
	ACC	$\downarrow$	0.15 ± 0.01		0.81 ± 0.06		0.46 ± 0.01
$\mathcal{G}_3$	ARI	$\downarrow$	0.03 ± 0.00		0.64 ± 0.12		0.12 ± 0.02
	NMI		$\underline{0.32 \pm 0.01}$		0.55 ± 0.05		0.18 ± 0.01
	ACC		0.17 ± 0.01	$\downarrow$	0.69 ± 0.22	$\downarrow$	0.43 ± 0.02
$\mathcal{G}_4$	ARI	$\downarrow$	0.03 ± 0.00	$\downarrow$	0.54 ± 0.24	$\downarrow$	0.08 ± 0.02
	NMI		$\underline{0.32 \pm 0.01}$	$\downarrow$	0.52 ± 0.08		0.17 ± 0.01
	ACC		0.17 ± 0.02		$\underline{0.86 \pm 0.01}$		$\underline{0.50 \pm 0.01}$
$\mathcal{G}_5$	ARI		$\underline{0.04 \pm 0.00}$		$\underline{0.69 \pm 0.01}$		$\underline{0.13 \pm 0.01}$
	NMI	$\downarrow$	0.31 ± 0.01		$\underline{0.57 \pm 0.01}$		$\underline{0.19 \pm 0.01}$

Table 11

Results of clustering nodes that belong to gold clusters whose size is greater or equal to 10 for $\mathcal{C}_0$ and all graphs. Average and standard deviation for each metric are computed on test folds during a 5-fold cross validation. Gray cells indicate the best result among clustering algorithms. Underlined values indicate the best result between graphs. $\downarrow$ indicates a lower value with regard to $\mathcal{G}_0$.

			Ward		Single		OPTICS
	ACC		0.14 ± 0.01		0.66 ± 0.17		0.25 ± 0.02
$\mathcal{G}_0$	ARI		0.02 ± 0.00		0.53 ± 0.22		0.02 ± 0.01
	NMI		0.29 ± 0.01		0.52 ± 0.06		$\underline{0.12 \pm 0.01}$
	ACC		$\underline{0.15 \pm 0.01}$		0.73 ± 0.10		0.25 ± 0.01
$\mathcal{G}_1$	ARI		0.02 ± 0.00		0.58 ± 0.13		0.02 ± 0.01
	NMI		$\underline{0.30 \pm 0.01}$	$\downarrow$	0.51 ± 0.03		$\underline{0.12 \pm 0.01}$
	ACC	$\downarrow$	0.12 ± 0.01	$\downarrow$	0.62 ± 0.16		$\underline{0.27 \pm 0.01}$
$\mathcal{G}_2$	ARI		0.02 ± 0.00	$\downarrow$	0.47 ± 0.19		$\underline{0.03 \pm 0.01}$
	NMI	$\downarrow$	0.26 ± 0.01	$\downarrow$	0.48 ± 0.05	$\downarrow$	0.11 ± 0.00
	ACC	$\downarrow$	0.12 ± 0.00		0.70 ± 0.18		0.26 ± 0.01
$\mathcal{G}_3$	ARI		0.02 ± 0.00		0.58 ± 0.23		$\underline{0.03 \pm 0.01}$
	NMI	$\downarrow$	0.28 ± 0.01		0.52 ± 0.06		$\underline{0.12 \pm 0.01}$
	ACC		0.14 ± 0.01	$\downarrow$	0.56 ± 0.18		0.25 ± 0.01
$\mathcal{G}_4$	ARI		0.02 ± 0.00	$\downarrow$	0.42 ± 0.20		0.02 ± 0.00
	NMI		0.29 ± 0.01	$\downarrow$	0.50 ± 0.06		$\underline{0.12 \pm 0.00}$
	ACC	$\downarrow$	0.13 ± 0.01		$\underline{0.74 \pm 0.15}$		$\underline{0.27 \pm 0.01}$
$\mathcal{G}_5$	ARI		0.02 ± 0.00		$\underline{0.61 \pm 0.16}$		$\underline{0.03 \pm 0.01}$
	NMI	$\downarrow$	0.28 ± 0.02		$\underline{0.54 \pm 0.06}$	$\downarrow$	0.11 ± 0.01

5.4. Distance analysis

During learning and clustering, our model is unaware of the different alignment relations holding between similar nodes. Indeed, the SNN loss only considers labels of gold clusters that do not indicate the alignment relations used to compute these clusters. This is particularly relevant for gold clusterings $\mathcal{C}_0$ and $\mathcal{C}_1$ that mix different alignment relations to compute the gold clusters. However, inspired by our preliminary results [26], we display in Figure 4 the distributions of distances between similar nodes in the test set by alignment relation. This analysis is presented for $\mathcal{C}_0$ and graphs $\mathcal{G}_0$ and $\mathcal{G}_5$. Interestingly, similarly to our preliminary results [26], such distributions of distances are coherent with the “strength” of the alignment relations. Indeed, for example, nodes that are weakly similar tend to be further apart than equivalent nodes. Only the `skos:broadMatch` relation presents different distance distributions with regard to the distance distributions of the other relations across the different test sets. This could be explained since this is the only non-symmetric relation (see Table 4).

6. Discussion

Table 6, Table 7, and Table 8 show that performance of clustering are generally better for gold clusterings $\mathcal{C}_2$ to $\mathcal{C}_6$ than $\mathcal{C}_0$ and $\mathcal{C}_1$. Recall that these two gold clusterings mix different alignment relations when computing gold clusters, and thus their matching task is expected to be more difficult. It can also be noticed that performance tends to decrease when considering additional gold clusters (*i.e.*, when decreasing their minimum size). Here again, such a task is more difficult. Indeed, clustering algorithms need to find more clusters (for Ward and Single), or clusters with a reduced minimum size (for OPTICS). However, this is not the case of $\mathcal{C}_2$, $\mathcal{C}_3$, and $\mathcal{C}_4$. This can be explained because, for such gold clusterings, only few gold clusters have a size greater or equal to 50 or 20 (see Figure 3), and thus only few training examples are available. Hence, reducing the minimum size leads to consider more training examples, and, despite the task being more difficult, improves performance.

Among the considered clustering algorithms, Single generally performs better than the others. For $\mathcal{C}_0$ and $\mathcal{C}_1$, OPTICS is the second best algorithm. For the other gold clusterings, Single and Ward give the best performance. In particular, we notice that OPTICS tends to have a decent ACC but reduced ARI and NMI. As this algorithm is unaware of the number of clusters to find and only knows their minimum size, low ARI and NMI may indicate a different clustering output in terms of both number and size of clusters. Indeed, ARI counts the pairs of nodes that have similar of different assignments both in predicted and gold clusters while NMI measures the mutual information between two different clusterings. On the contrary, ACC counts the number of nodes correctly assigned. Hence, big gold clusters (partially) correctly assigned may increase the ACC value even between different clusterings. Such a situation arises here since some of our gold clusterings lead to gold clusters with numerous nodes. For example, Figure 3 shows that a gold cluster in $\mathcal{C}_0$ contains 17,568 nodes.

Table 6, Table 7, and Table 8 allow to compare results between $\mathcal{G}_0$, *i.e.*, no inference rules, and $\mathcal{G}_5$, *i.e.*, all inference rules. It appears that $\mathcal{G}_5$ generally increases performance for $\mathcal{C}_0$ and $\mathcal{C}_1$. Results for the other gold clusterings do not show such an homogeneous and important increase in performance between $\mathcal{G}_0$ and $\mathcal{G}_5$. As aforementioned, $\mathcal{C}_0$ and $\mathcal{C}_1$ mix different alignment relations, which leads to a more difficult matching task. Hence, our results indicate that inference rules associated with domain knowledge provide useful improvements when dealing with heterogeneous similarities and clusters. It is frequent in matching task to consider different alignment relations or "levels" of similarity. Hence, matching approaches could benefit from taking into account inference rules to improve matching results.

Results for $\mathcal{C}_0$ in Table 9, Table 10, and Table 11 detail the clustering performance for each graph transformation. Performances for Ward do not present noticeable modifications. For Single and OPTICS, inference rules seem to mostly improve results, except for $\mathcal{G}_4$. This graph contains all the instantiation links that can be inferred. Consequently, "general" classes are directly linked to entities that instantiate them instead of indirectly. For example, in Table 3, k is directly linked to i instead of indirectly. Hence, when computing the embeddings of such entities, embeddings of both general and specific classes are directly considered through the same predicate `type`, which makes difficult for GCNs to weight these classes differently. As specific classes are more important than general classes to discriminate similar and dissimilar nodes, their undifferentiated influence in embeddings may explain the decrease in performance. We notice that $\mathcal{G}_5$ performs best, which advocates for considering all inference rules together. However, based on the degraded performance of $\mathcal{G}_4$ with regard to $\mathcal{G}_0$, one may want to solely focus on inference rules represented by $\mathcal{G}_1$, $\mathcal{G}_2$, and $\mathcal{G}_3$. As expected from the first three tables, Table 9, Table 10, and Table 11 also confirm that Single is the best performing clustering algorithm for $\mathcal{C}_0$, even across the different graph transformations.

Regarding the distance analysis of node embeddings, Figure 4 shows that distances between similar nodes are different depending on the alignment relation holding between them. Recall that our GCN model is agnostic to these alignment relations when computing the SNN loss. Interestingly, distances reflect the "strength" of the alignment relations: strong similarities (*i.e.*, `owl:sameAs` and `skos:closeMatch` links) have smaller distances than weaker ones (*i.e.*, `skos:relatedMatch` and `skos:related` links). The `skos:broadMatch` relation appears more difficult to position with regard to others. This can be explained as it is the only alignment relation that is not symmetric. Such coherent distributions of

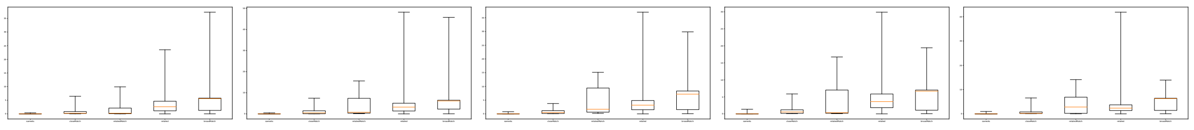

(a) $\mathcal{G}_0$ – Fold 1 (b) $\mathcal{G}_0$ – Fold 2 (c) $\mathcal{G}_0$ – Fold 3 (d) $\mathcal{G}_0$ – Fold 4 (e) $\mathcal{G}_0$ – Fold 5

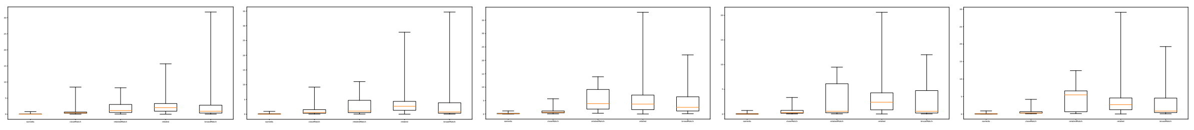

(f) $\mathcal{G}_5$ – Fold 1 (g) $\mathcal{G}_5$ – Fold 2 (h) $\mathcal{G}_5$ – Fold 3 (i) $\mathcal{G}_5$ – Fold 4 (j) $\mathcal{G}_5$ – Fold 5

Fig. 4. Distributions of distances between similar nodes by alignment relation for each test set, the $\mathcal{C}_0$ gold clustering and the two graphs $\mathcal{G}_0$ and $\mathcal{G}_5$. In each subpicture, links are from left to right: `owl:sameAs`, `skos:closeMatch`, `skos:relatedMatch`, `skos:related`, and `skos:broadMatch`.

distances seem to indicate the "rediscovery" of alignment relations by GCNs and encourage to consider the distance between embeddings of nodes in a "semantic" way, *i.e.*, smaller distances indicate stronger similarities. Additionally, such different distances also seem to confirm that the neighborhood aggregation of embeddings in GCNs makes them well-suited to a structural and relational matching.

Our results highlight the interest of considering formal semantics associated with knowledge graphs in embedding approaches and seem to advocate for a further integration of formal semantics within embedding models. Future works may investigate the same targets with different embedding techniques, whether based on graph neural networks [31] or others (*e.g.*, translational approaches such as TransE). Additionally, we did not use attention mechanisms, which could also consider formal semantics as in Logic Attention Network [24]. Here, inference rules associated with domain knowledge are used to transform the knowledge graph as a pre-processing operation. However, we could envision to consider such mechanisms directly in the model (*e.g.*, weight sharing between predicates and their super-predicates). Literals could also be taken into account [9]. In a larger perspective, one major future work lies in investigating if and how other semantics than types of similarity links can emerge in the output embedding space.

7. Conclusion

In this paper, we proposed to match entities of a knowledge graph by learning node embeddings with Graph Convolutional Networks (GCNs) and clustering nodes based on their embeddings. We particularly investigated the interplay between formal semantics associated with knowledge graphs and GCN models. Our results showed that considering inference rules associated with domain knowledge tends to improve performance. Additionally, even if our GCN model was agnostic to the exact alignment relations holding between entities (*e.g.*, equivalence, weak similarity), distances in the embedding space are coherent with the "strength" of the alignment relations. These results seem to advocate for a further integration of formal semantics within embedding models.

Acknowledgements

This work was supported by the *PractiKPharma* project, founded by the French National Research Agency (ANR) under Grant ANR15-CE23-0028, and by the *Snowball* Inria Associate Team.

References

[1] T. Berners-Lee, J. Hendler, O. Lassila et al., The Semantic Web, *Scientific american* **284**(5) (2001), 28–37.
[2] J. Euzenat and P. Shvaiko, *Ontology Matching, Second Edition*, Springer, 2013. ISBN 978-3-642-38720-3.

[3] T.R. Gruber, A translation approach to portable ontology specifications, *Knowledge acquisition* **5**(2) (1993), 199–220.

[4] H. Cai, V.W. Zheng and K.C. Chang, A Comprehensive Survey of Graph Embedding: Problems, Techniques, and Applications, *IEEE Trans. Knowl. Data Eng.* **30**(9) (2018), 1616–1637. doi:10.1109/TKDE.2018.2807452.

[5] T.N. Kipf and M. Welling, Semi-Supervised Classification with Graph Convolutional Networks, in: *5th International Conference on Learning Representations, ICLR 2017, Toulon, France, April 24-26, 2017, Conference Track Proceedings*, OpenReview.net, 2017.

[6] M.S. Schlichtkrull, T.N. Kipf, P. Bloem, R. van den Berg, I. Titov and M. Welling, Modeling Relational Data with Graph Convolutional Networks, in: *The Semantic Web - 15th International Conference, ESWC 2018, Heraklion, Crete, Greece, June 3-7, 2018, Proceedings*, Lecture Notes in Computer Science, Vol. 10843, Springer, 2018, pp. 593–607. doi:10.1007/978-3-319-93417-4_38.

[7] R.V. Guha, Towards A Model Theory for Distributed Representations, in: *2015 AAAI Spring Symposia, Stanford University, Palo Alto, California, USA, March 22-25, 2015*, AAAI Press, 2015. http://www.aaai.org/ocs/index.php/SSS/SSS15/paper/view/10220.

[8] N. Pang, W. Zeng, J. Tang, Z. Tan and X. Zhao, Iterative Entity Alignment with Improved Neural Attribute Embedding, in: *Proceedings of the Workshop on Deep Learning for Knowledge Graphs (DL4KG2019) Co-located with the 16th Extended Semantic Web Conference 2019 (ESWC 2019), Portoroz, Slovenia, June 2, 2019*, CEUR Workshop Proceedings, Vol. 2377, CEUR-WS.org, 2019, pp. 41–46.

[9] Z. Wang, Q. Lv, X. Lan and Y. Zhang, Cross-lingual Knowledge Graph Alignment via Graph Convolutional Networks, in: *Proceedings of the 2018 Conference on Empirical Methods in Natural Language Processing, Brussels, Belgium, October 31 - November 4, 2018*, Association for Computational Linguistics, 2018, pp. 349–357. doi:10.18653/v1/d18-1032.

[10] P. Monnin, M. Couceiro, A. Napoli and A. Coulet, Knowledge-Based Matching of n-ary Tuples, in: *Ontologies and Concepts in Mind and Machine - 25th International Conference on Conceptual Structures, ICCS 2020, Bolzano, Italy, September 18-20, 2020, Proceedings*, M. Alam, T. Braun and B. Yun, eds, Lecture Notes in Computer Science, Vol. 12277, Springer, 2020, pp. 48–56. doi:10.1007/978-3-030-57855-8_4.

[11] H. Paulheim, Knowledge graph refinement: A survey of approaches and evaluation methods, *Semantic Web* **8**(3) (2017), 489–508. doi:10.3233/SW-160218.

[12] M. Whirl-Carrillo, E.M. McDonagh, J.M. Hebert, L. Gong, K. Sangkuhl, C.F. Thorn, R.B. Altman and T.E. Klein, Pharmacogenomics knowledge for personalized medicine, *Clinical pharmacology and therapeutics* **92**(4) (2012), 414.

[13] K.E. Caudle et al., Incorporation of Pharmacogenomics into Routine Clinical Practice: the Clinical Pharmacogenetics Implementation Consortium (CPIC) Guideline Development Process, *Current Drug Metabolism* **15**(2) (2014), 209–217.

[14] A. Coulet and M. Smaïl-Tabbone, Mining Electronic Health Records to Validate Knowledge in Pharmacogenomics, *ERCIM News* **2016**(104) (2016).

[15] N. Noy, A. Rector, P. Hayes and C. Welty, Defining N-ary Relations on the Semantic Web, *W3C working group note* **12**(4) (2006).

[16] P. Monnin, J. Legrand, G. Husson, P. Ringot, A. Tchechmedjiev, C. Jonquet, A. Napoli and A. Coulet, PGxO and PGxLOD: a reconciliation of pharmacogenomic knowledge of various provenances, enabling further comparison, *BMC Bioinformatics* **20-S**(4) (2019), 139:1–139:16. doi:10.1186/s12859-019-2693-9.

[17] Q. Wang, Z. Mao, B. Wang and L. Guo, Knowledge Graph Embedding: A Survey of Approaches and Applications, *IEEE Trans. Knowl. Data Eng.* **29**(12) (2017), 2724–2743. doi:10.1109/TKDE.2017.2754499.

[18] M. Nickel, K. Murphy, V. Tresp and E. Gabrilovich, A Review of Relational Machine Learning for Knowledge Graphs, *Proceedings of the IEEE* **104**(1) (2016), 11–33. doi:10.1109/JPROC.2015.2483592.

[19] A. Bordes, N. Usunier, A. García-Durán, J. Weston and O. Yakhnenko, Translating Embeddings for Modeling Multi-relational Data, in: *Advances in Neural Information Processing Systems 26: 27th Annual Conference on Neural Information Processing Systems 2013. Proceedings of a meeting held December 5-8, 2013, Lake Tahoe, Nevada, United States*, 2013, pp. 2787–2795.

[20] P. Ristoski and H. Paulheim, RDF2Vec: RDF Graph Embeddings for Data Mining, in: *The Semantic Web - ISWC 2016 - 15th International Semantic Web Conference, Kobe, Japan, October 17-21, 2016, Proceedings, Part I*, Lecture Notes in Computer Science, Vol. 9981, 2016, pp. 498–514. doi:10.1007/978-3-319-46523-4_30.

[21] N. Frosst, N. Papernot and G.E. Hinton, Analyzing and Improving Representations with the Soft Nearest Neighbor Loss, in: *Proceedings of the 36th International Conference on Machine Learning, ICML 2019, 9-15 June 2019, Long Beach, California, USA*, Proceedings of Machine Learning Research, Vol. 97, PMLR, 2019, pp. 2012–2020.

[22] H. Paulheim, Make Embeddings Semantic Again!, in: *Proceedings of the ISWC 2018 Posters & Demonstrations, Industry and Blue Sky Ideas Tracks co-located with 17th International Semantic Web Conference (ISWC 2018), Monterey, USA, October 8th - to - 12th, 2018*, CEUR Workshop Proceedings, Vol. 2180, CEUR-WS.org, 2018.

[23] L. Serafini and A.S. d'Avila Garcez, Logic Tensor Networks: Deep Learning and Logical Reasoning from Data and Knowledge, in: *Proceedings of the 11th International Workshop on Neural-Symbolic Learning and Reasoning (NeSy'16) co-located with the Joint Multi-Conference on Human-Level Artificial Intelligence (HLAI 2016), New York City, NY, USA, July 16-17, 2016*, CEUR Workshop Proceedings, Vol. 1768, CEUR-WS.org, 2016.

[24] P. Wang, J. Han, C. Li and R. Pan, Logic Attention Based Neighborhood Aggregation for Inductive Knowledge Graph Embedding, in: *The Thirty-Third AAAI Conference on Artificial Intelligence, AAAI 2019, The Thirty-First Innovative Applications of Artificial Intelligence Conference, IAAI 2019, The Ninth AAAI Symposium on Educational Advances in Artificial Intelligence, EAAI 2019, Honolulu, Hawaii, USA, January 27 - February 1, 2019*, AAAI Press, 2019, pp. 7152–7159. doi:10.1609/aaai.v33i01.33017152.

[25] V. Gutiérrez-Basulto and S. Schockaert, From Knowledge Graph Embedding to Ontology Embedding? An Analysis of the Compatibility between Vector Space Representations and Rules, in: *Principles of Knowledge Representation and Reasoning: Proceedings of the Sixteenth International Conference,*

KR 2018, Tempe, Arizona, 30 October - 2 November 2018, AAAI Press, 2018, pp. 379–388.

[26] P. Monnin, C. Raïssi, A. Napoli and A. Coulet, Knowledge Reconciliation with Graph Convolutional Networks: Preliminary Results, in: *Proceedings of the Workshop on Deep Learning for Knowledge Graphs (DL4KG2019) Co-located with the 16th Extended Semantic Web Conference 2019 (ESWC 2019), Portoroz, Slovenia, June 2, 2019*, CEUR Workshop Proceedings, Vol. 2377, CEUR-WS.org, 2019, pp. 47–56.

[27] F. Pedregosa, G. Varoquaux, A. Gramfort, V. Michel, B. Thirion, O. Grisel, M. Blondel, P. Prettenhofer, R. Weiss, V. Dubourg, J. Vanderplas, A. Passos, D. Cournapeau, M. Brucher, M. Perrot and E. Duchesnay, Scikit-learn: Machine Learning in Python, *Journal of Machine Learning Research* **12** (2011), 2825–2830.

[28] M. Ankerst, M.M. Breunig, H. Kriegel and J. Sander, OPTICS: Ordering Points To Identify the Clustering Structure, in: *SIGMOD 1999, Proceedings ACM SIGMOD International Conference on Management of Data, June 1-3, 1999, Philadelphia, Pennsylvania, USA*, ACM Press, 1999, pp. 49–60. doi:10.1145/304182.304187.

[29] F. Baader et al.(eds), *The Description Logic Handbook: Theory, Implementation, and Applications*, Cambridge University Press, 2003.

[30] D.P. Kingma and J. Ba, Adam: A Method for Stochastic Optimization, in: *3rd International Conference on Learning Representations, ICLR 2015, San Diego, CA, USA, May 7-9, 2015, Conference Track Proceedings*, 2015.

[31] V.P. Dwivedi, C.K. Joshi, T. Laurent, Y. Bengio and X. Bresson, Benchmarking Graph Neural Networks, *CoRR* **abs/2003.00982** (2020).